Electronic supporting information

Resolving a structural issue in cerium-nickel-based oxide: single compound or a two-phase system?

Jelena Kojčinović[a], Dalibor Tatar[a], Stjepan Šarić[a], Cora Bartus Pravda[b], Andraž Mavrič[c], Iztok Arčon[c,d], Zvonko Jagličić[e,f], Maximilian Mellin[g], Marcus Einert[g], Angela Altomare[h], Rocco Caliandro[h], Ákos Kukovecz[b], Jan Philipp Hofmann[g] and Igor Djerdj[a, *]

a. *Department of Chemistry, Josip Juraj Strossmayer University of Osijek, Cara Hadrijana 8/A, 31000 Osijek, Croatia*

b. *Department of Applied and Environmental Chemistry, University of Szeged, 6720 Szeged, Hungary*

c. *University of Nova Gorica, Vipavska 13, 5000 Nova Gorica, Slovenia*

d. *Institute Jožef Stefan, Jamova 39, 1000 Ljubljana, Slovenia*

e. *Institute of Mathematics, Physics, and Mechanics, University of Ljubljana, Jamova 2, 1000 Ljubljana, Slovenia*

f. *Faculty of Civil & Geodetic Engineering, University of Ljubljana, Jadranska 19, 1000 Ljubljana, Slovenia*

g. *Surface Science Laboratory, Department of Materials and Earth Sciences, Technical University of Darmstadt, Otto-Berndt-Strasse 3, 64287 Darmstadt, Germany*

h. *Institute of Crystallography, CNR, via Amendola 122/o, Bari 70126, Italy*

* igor.djerdj@kemija.unios.hr

Table S1. Amounts of precursors for the synthesis of compounds.

Compound	Element	Amount (mmol)
RB1 ($CeNiO_3$)	Ce	1
	Ni	
CeO_2	Ce	1
NiO	Ni	1

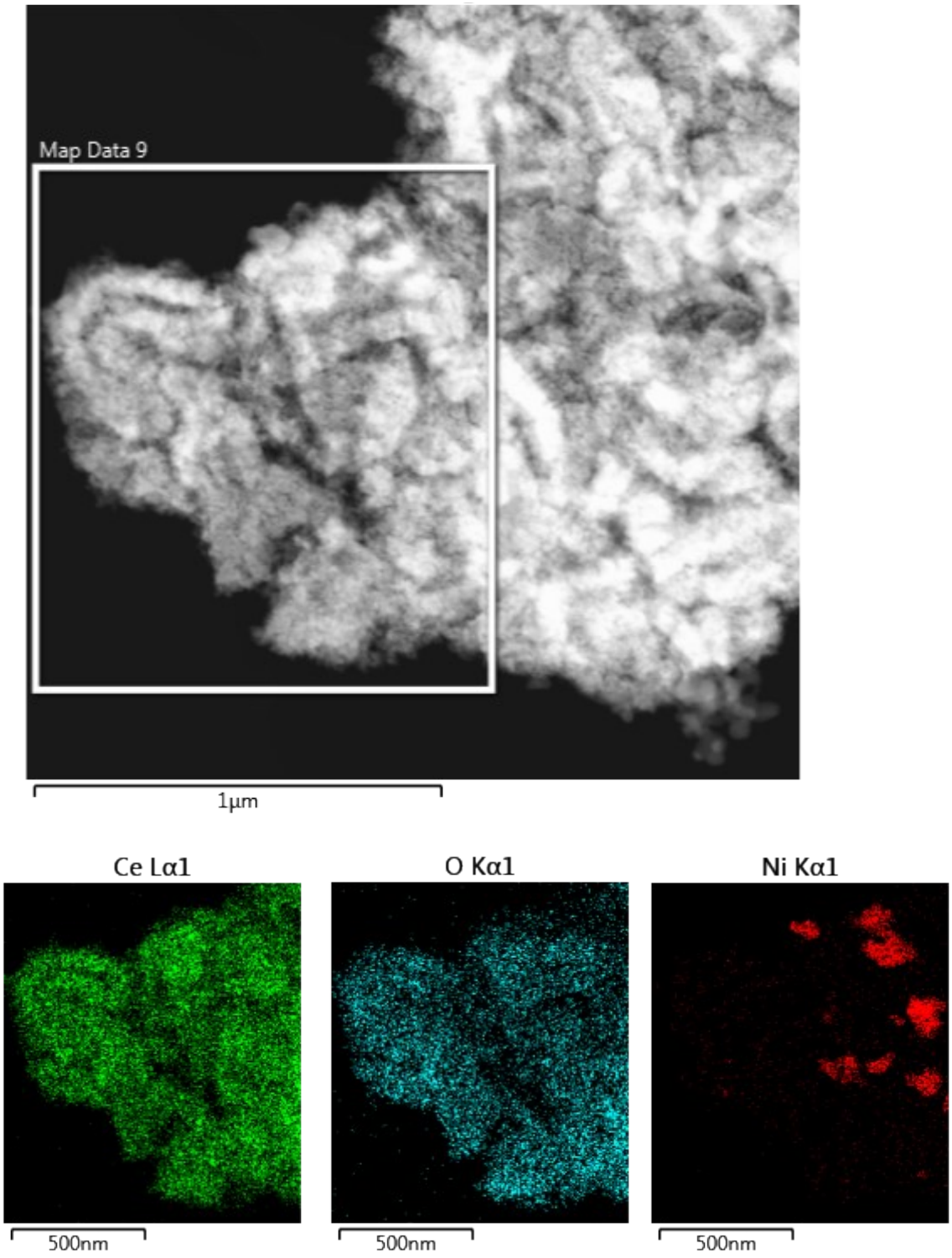

Figure S1. STEM-EDS image of a mixture CeO_2 + NiO (n : n = 1:1) at one spot showing a non-uniform distribution of Ce, Ni and O. The measured spot contains more cerium than nickel.

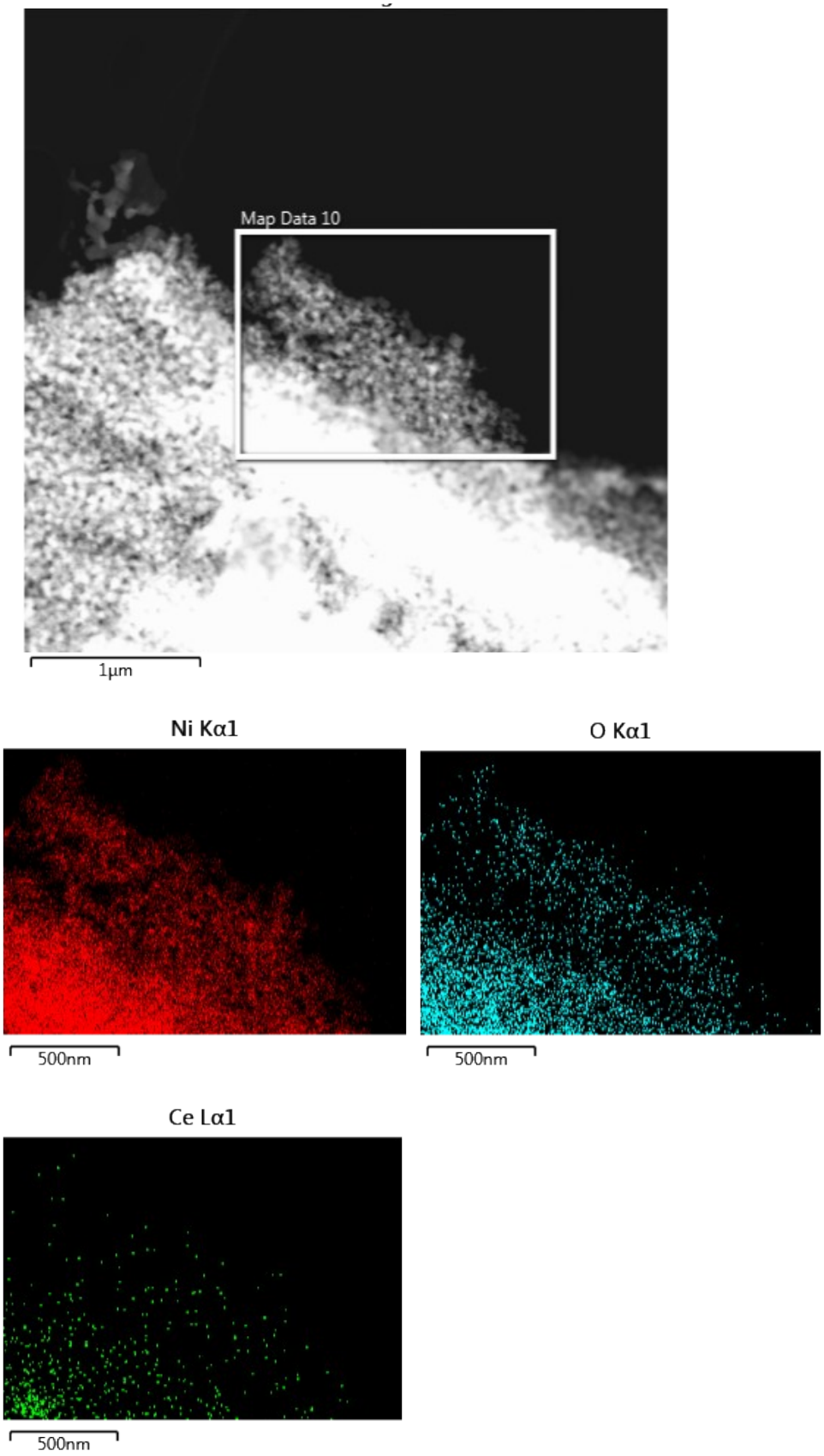

Figure S2. STEM-EDS image of a mixture CeO_2 + NiO (n : n = 1:1) at one spot showing a non-uniform distribution of Ce, Ni and O.The measured spot contains more nickel than cerium.

EXAFS analysis of CeO_2 and RB1 at Ce L_3-edge

Structural parameters of the average local Ce neighbourhood (the type and the average number of neighbours; the radii and Debye–Waller factor of neighbour shells) in CeO_2 are quantitatively resolved from the EXAFS spectra by comparing the measured EXAFS signal with the model signal. The FEFF model for the crystalline CeO_2 nanoparticles is based on the cubic crystal structure of CeO_2 with the space group *Fm*–3*m* with the lattice constant a = 5.411 Å (PDF4+ database card #00-004-0593), where Ce is coordinated with 8 oxygen atoms at a distance of 2.34 Å, 12 Ce atoms at 3.83 Å and 24 oxygen atoms at 4.47 Å. The FEFF model comprised three single scattering and ten significant multiple scattering paths up to 4.6 Å, with 7 variable parameters: coordination shell distance (R) for the first (O) and second (Ce) neighbour shell, Debye–Waller factor (σ^2) of the single scattering path for (Ce-O) whereas Debye–Waller factors of other paths are evaluated using Debye model via Debye temperature (θ_d). The amplitude reduction factor (S_0^2) and shift of the energy origin of the photoelectron (ΔE_o), common to all scattering paths, are introduced. The shell coordination numbers were fixed to the crystallographic values in the fit, and the structural parameters of multiple scattering paths are constrained to those of the corresponding single scattering paths. A very good EXAFS fit (**Fig. S3**) is obtained in the k range of 2–9.9 Å and the R-range of 1.3–4.6 Å. The best-fit structural parameters are given in **Table S2**. For the RB1 sample, the EXAFS spectra were fitted with the FEFF model as it was done for CeO_2 (cubic *Fm*–3*m*) and the FEFF model for CeO_2 with the space group $P4_2/nmc$ with the lattice constant a = 3.818 Å, b = 3.818 Å and c = 5.426 Å (PDF4+ database card #04-025-2756). For fitting the RB1, the amplitude reduction factor (S_0^2) was fixed to the value obtained for CeO_2 and shell coordination numbers were used as variable parameters. The best-fit structural parameters are given in **Table S2**. The results show that EXAFS cannot resolve between cubic and tetragonal structures for RB1 sample. The obtained structural parameters for RB1 are the same for both FEFF models and in agreement with those obtained for CeO_2.

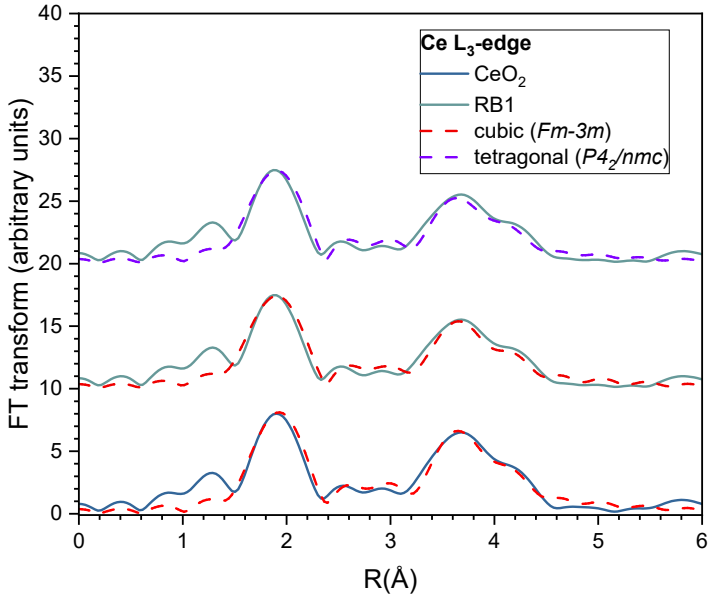

Figure S3. Fourier transform magnitude of the k^3-weighted Ce L_3-edge EXAFS spectra of the CeO_2 and RB1 samples calculated in the k range of 2–9.9 Å. Experiment – (solid line); the best fit EXAFS model calculated in the R-range of 1.3 to 4.6Å – (red dashed line for cubic system, violet dashed line for tetragonal system). Graph curves shifted vertically for clarity.

Table S2. Parameters of the nearest coordination shells around Ce cations in the CeO_2 and RB1 sample: coordination number (N), distance (R), and Debye-Waller factor (σ^2). Uncertainty of the last digit is given in parentheses. The best fit is obtained with the amplitude reduction factor $S_0^2 = 0.66$ and the shift of the energy origin $\Delta E_o = 8(1)$ eV.

CeO_2				
Neighbour	N (fixed)	R (Å)	σ^2 (Å^2)	R-factor
O	8	2.34(1)	0.004(3)	0.028
Ce	12	3.86(1)	0.004(3)	
O	24	4.41(1)	0.02(1)	
RB1 - fit with cubic *Fm–3m* structure model				
Neighbour	N	R (Å)	σ^2 (Å^2)	R-factor
O	8(2)	2.33(1)	0.006(3)	0.041
Ce	10(3)	3.85(1)	0.004(3)	
O	21(7)	4.41(2)	0.02(1)	
RB1 - fit with tetragonal *P4$_2$/nmc* structure model				
Neighbour	N	R (Å)	σ^2 (Å^2)	R-factor
O	8(2)	2.35(1)	0.005(3)	0.042
Ce	8(3)	3.86(1)	0.004(3)	
O	20(8)	4.3(1)	0.03(1)	

Table S3. High-resolution Ce 3d spectra peak position analysis for CeO_2 and RB1.

CeO_2	RB1	Assignment	Orbital splitting
Binding energy (eV)	**Binding energy (eV)**		
883.1	883.3	Core level	$3d_{5/2}$
889.8	890.1	Satellite 1	
899.3	899.3	Satellite 2	
902.3	901.9	Core level	$3d_{3/2}$
908.8	908.7	Satellite 3	
917.8	918.4	Satellite 4	

Table S4. High-resolution Ni 2p spectra peak position analysis for NiO and RB1.

NiO	RB1	Assignment	Orbital splitting
Binding energy (eV)	**Binding energy (eV)**		
853.9	854.4	Core level	$2p_{3/2}$
855.7	855.8	Core level	
861.0	857.3	Satellite 1	
864.4	861.4	Satellite 2	
866.6	864.1	Core level	$2p_{1/2}$
871.4	Not possible to read	Core level	
873.2	874.0	Core level	
879.3	Not possible to read	Satellite 3	

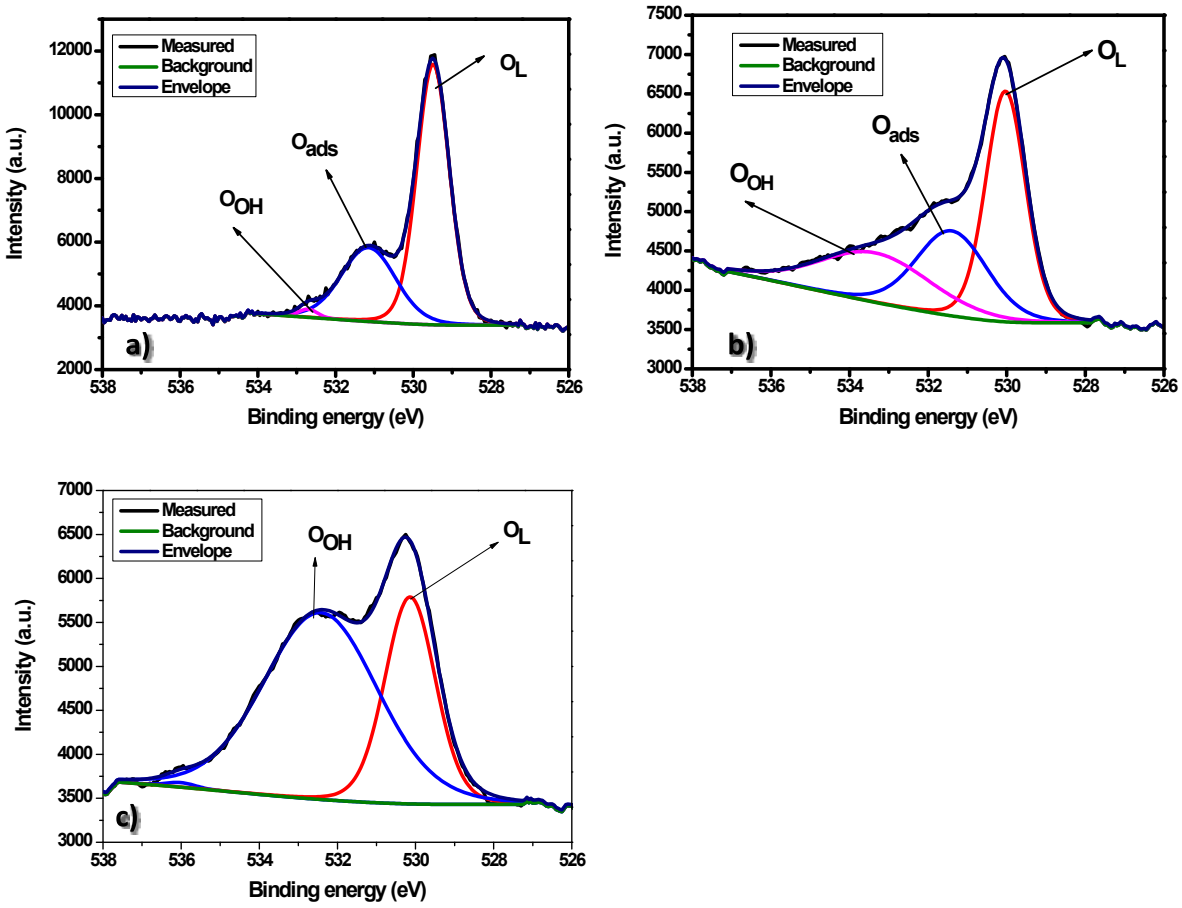

Figure S4. Deconvoluted high-resolution O 1s spectrum of a) NiO b) CeO_2 and c) RB1.

Table S5. Deconvoluted O 1s spectra report for CeO_2, NiO and RB1.

NiO		CeO_2		RB1		Assignment
Binding energy (eV)	**Area**	**Binding energy (eV)**	**Area**	**Binding energy (eV)**	**Area**	
529.5	8909.8	530.03	3902.3	530.1	3977.2	Lattice oxygen (O_L)
531.2	4252.8	531.4	2554.4	-	-	Adsorbed oxygen species (O_{ads})
532.7	161.7	533.3	2347.0	532.4	8113.3	Hydroxides (O_{OH})
Total area	**13324.2**		**8803.7**		**12142.1**	
Oxygen species concentration	**31.9 %**		**29.0 %**		-	
Hydroxide concentration	**1.2 %**		**26.7 %**		**66.8 %**	

.

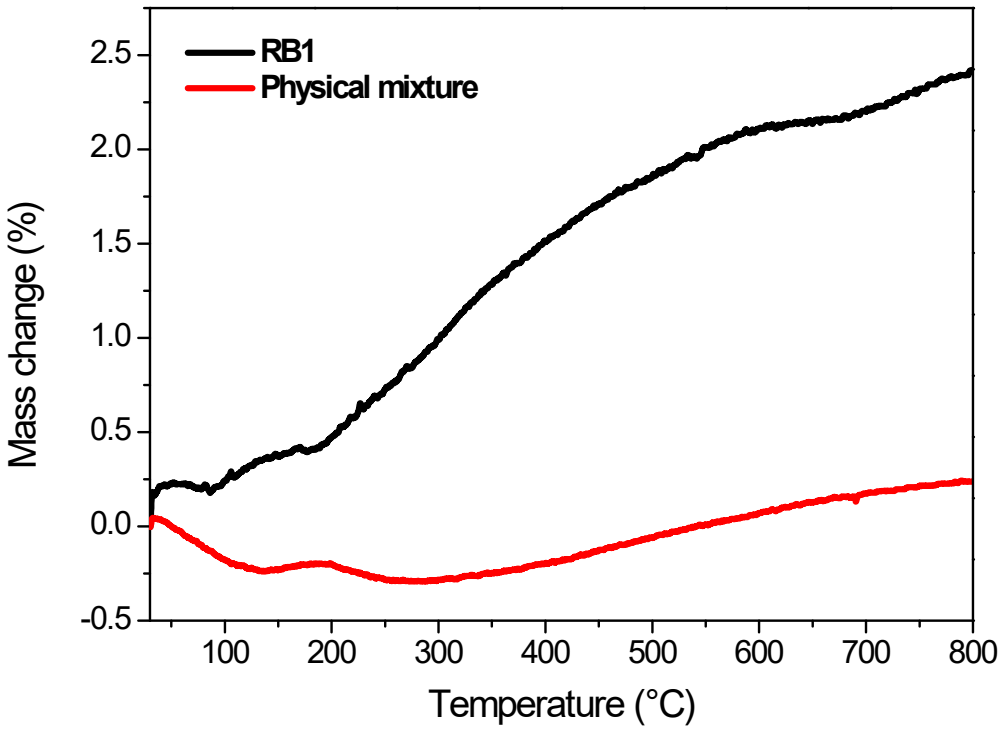

Figure S5. Thermogravimetric curves of RB1 (black) and a physical mixture of CeO_2 + NiO (red) during heating in an oxidative atmosphere (10 °C/min) from 30 °C to 800 °C.

Table S6. Crystallographic data obtained from the Rietveld refinement of 3% Ni doped CeO_2.

Compound	**CeO_2 (3% doped Ni)**
Chemical formula	**$Ce_{0.97}Ni_{0.03}O_2$**
Crystal system	Tetragonal
Space group	$P\,4_2\,/\,n\,m\,c$
Z	2
Calculated density (g/cm^3)	7.076
Unit cell parameters (Å)	a= 3.8319(2) c= 5.4183(1)
Unit cell volume (Å^3)	79.5600(1)
Phase content (wt. %)	100
Average crystallite size (nm)	8.5
Average apparent microstrain ($\times10^{-4}$)	0.95
R_B	5.58
R_p, R_{wp}, R_e	13.2, 10.7, 8.23
χ^2	1.68